Biosensors and Bioelectronics 25 (2010) 2009–2015

Contents lists available at ScienceDirect

Biosensors and Bioelectronics

journal homepage: www.elsevier.com/locate/bios

Electrospun hemoglobin microbelts based biosensor for sensitive detection of hydrogen peroxide and nitrite

Yu Ding[a], Ying Wang[a], Baikun Li[b], Yu Lei[a,*]

[a] Department of Chemical, Materials, and Biomolecular Engineering, University of Connecticut, 191 Auditorium Rd, Storrs, CT 06269-3222, USA
[b] Department of Civil and Environmental Engineering, University of Connecticut, Storrs, CT 06269, USA

ARTICLE INFO

Article history:
Received 7 November 2009
Received in revised form
29 December 2009
Accepted 21 January 2010
Available online 1 February 2010

Keywords:
Hemoglobin
Electrospinning
Microbelts
Hydrogen peroxide
Nitrite
Biosensor

ABSTRACT

Highly porous hemoglobin (Hb) microbelts based biosensor was developed by directly electrospinning Hb onto the glassy carbon (GC) electrode surface without using immobilization matrix, offering an excellent electrochemical sensing platform. Ultraviolet–visible spectroscopy and Fourier transform infrared spectroscopy were performed to demonstrate that Hb still kept its native structure in the as-electrospun microbelts. The electrocatalytic property of Hb microbelts modified GC electrode was investigated using hydrogen peroxide (H_2O_2) and nitrite as model compounds. The cyclic voltammetry results have demonstrated that the Hb microbelts modified electrode shows enhanced activity in the electrochemical reduction of H_2O_2 and nitrite, which offers a number of attractive features and is explored to develop an amperometric biosensor. The Hb microbelts based amperometric biosensor has fast responses to H_2O_2 and nitrite, good dynamic response ranges, excellent detection limits of 0.61 μM for H_2O_2 and 0.47 μM for nitrite (S/N = 3), and superior $K_{M,app}$ values of 0.093 mM for H_2O_2 and 0.713 mM for nitrite, respectively. These results demonstrate that the electrospun Hb microbelts can significantly enhance the direct electrochemistry of Hb and has great potential application in mediator-free biosensor applications.

1. Introduction

In recent years, there are growing research interests in the direct electrochemistry of redox proteins because of its great importance in realizing the mechanisms of electron transfer in real biological systems as well as its potential application in fabricating mediator-free and sensitive biosensors (He and Zhu, 2006; Shan et al., 2007). Among various redox proteins such as cytochrome *c*, glucose oxidase, horseradish peroxidase, hemoglobin, and myoglobin, hemoglobin (Hb) has been extensively studied (Armstrong et al., 1988; Qiao et al., 2008; Yu and Ju, 2003; Zhang, 2008; Zhao et al., 2006a, 2008). Hb is tetrameric protein consisting of four subunits and each subunit is a combination of a polypeptide chain and a heme. The heme consists of an iron atom (Fe^{2+} or Fe^{3+}) attached to a planar organic structure belonging to porphyrin compounds. In Hb, each heme group serves as the active site to which a molecule of oxygen may be bound and also offers Hb the ability to reduce different targets such as H_2O_2 and nitrite. Hb is regarded as an ideal model molecule for electron-transfer study between redox protein and electrode and has been widely applied in the development of biosensors owing to its known and documented structure, commercial availability and moderate cost (He and Zhu, 2006). However, it is difficult to transfer electrons from Hb to conventional electrodes due to various factors such as the deep burying of heme groups in the large three-dimensional structure of the proteins with the associated low accessibility of analyte molecules and the denaturation of Hb when immobilized onto the electrode surface. In order to enhance the direct electrochemistry of Hb and the sensitivity of Hb based biosensors, different immobilization materials, such as hydrogel polysaccharide (Liu et al., 2004), amphiphilic polymer (Sun et al., 2000), mesopore-structured organic peroxide (Jian et al., 2007), and lipids (Han et al., 2002) have been reported to provide suitable microenvironment for Hb and construct a Hb hybrid film with enhanced adherent ability to the surface of electrode. Even though these immobilization methods are elegant, hemoglobins are either entrapped in the materials or adsorbed in the mesopores. Thus, the additional diffusion resistance offered by the entrapment materials or the mesopores usually results in lower sensitivity and higher detection limit. With the development of nanotechnology, various nanoparticles such as Au (Maduralveeran and Ramaraj, 2007), Ag (Zhao et al., 2006a), quantum dots (Cai et al., 2008), $CaCO_3$ (Shan et al., 2007), and clay (Liu et al., 2005), and various nanotubes such as TiO_2 nanotubes (Gao et al., 2008), silica nanotubes (Kapoor et al., 2009) and carbon nanotubes (Cai and Chen, 2004) have also been exploited to offer a large surface for Hb adsorption and/or to facilitate direct electron transfer between Hb and elec-

* Corresponding author. Tel.: +1 860 486 4554; fax: +1 860 486 2959.
E-mail address: ylei@engr.uconn.edu (Y. Lei).

0956-5663/$ – see front matter © 2010 Elsevier B.V. All rights reserved.
doi:10.1016/j.bios.2010.01.024

trode, resulting in various Hb based biosensors for H_2O_2 and/or nitrite. However, these nanomaterials cannot stand alone and usually a matrix is required to entrap them for electrode attachment. Recently electrospun continuous nano- and microstructured membranes have attracted more attention than other porous materials in sensor and biosensor development due to their inherent large specific surface area and highly porous structure (Jia et al., 2009; Wang et al., 2009a,b), which facilitate the adsorption/desorption process and minimize the diffusion resistance of molecules to the surface of materials (Ding et al., 2009; Yoon et al., 2009). In this paper, Hb was directly electrospun onto the surface of glassy carbon (GC) electrode with highly porous structure, which can significantly reduce the additional diffusion resistance of analytes. It can also attach to the electrode surface without the help of an entrapment matrix. UV–vis and FT-IR spectra indicated that Hb in the as-electrospun microbelts retained its native structure. Direct electrochemistry of Hb microbelts modified GC electrode and its applications in sensitive detection of H_2O_2 and nitrite were extensively investigated. Due to the extremely small thickness and the large surface area of the as-prepared Hb microbelts, direct electron transfer between Hb and electrode and the electrocatalytic activity of Hb microbelts modified electrode can be significantly enhanced. Thus sensitive detection of H_2O_2 and nitrite is achieved.

2. Experimental

2.1. Reagents

Hb (64.5 kDa) from bovine blood was purchased from MP Biomedicals. 2,2,2-Trifluoroethanol (TFE) and H_2O_2 (30 wt%) were obtained from Fisher Scientific. 0.1 M phosphate buffer solutions with various pH values were prepared by mixing stock standard solutions of Na_2HPO_4 and NaH_2PO_4 and adjusting the pH values with NaOH or H_3PO_4 solutions. 0.05 M pH 4.0 Britton–Robinson (BR) buffer was prepared using phosphoric, acetic and boric acids and the pH was adjusted by the addition of NaOH solution. Deionized (DI) water (18.2 MΩ cm) generated by a Barnstead water system was used to prepare aqueous solutions.

2.2. Fabrication of Hb microbelts modified GC electrode

Before surface modification, the GC electrode (dia. 3 mm) was polished with 1 μm and 0.05 μm alumina slurries sequentially, and then rinsed with DI water thoroughly. Finally, the electrode was sonicated in ethanol and DI water, respectively, followed by drying at room temperature. The modification of GC electrode by electrospun Hb microbelts is shown in Fig. 1S. Briefly, a GC electrode was inserted vertically in the body of plastic foam until its surface reached the same level as the upper surface of the plastic foam. Then the whole surface was covered by alumina foil with an open hole in the center. The hole has the same size as that of GC electrode and thus exposes the electrode surface to environment. Next, Hb was dissolved in TFE to prepare a 175 mg/mL solution and was electrospun using a 19 gauge needle with a flow rate of 1.8 mL/h at an applied potential of 22.5 kV with a collection distance of 12 cm. After 10 min electrospinning, a thin film of Hb microbelts was formed on the surface of GC electrode. The Hb microbelts modified electrode was then placed in glutaraldehyde vapor for crosslinking to make the Hb microbelts film water-insoluble. Before the use of Hb microbelts modified GC electrode, it was immersed in pH 7.0 phosphate buffer at 4 °C for at least 2 h to wet Hb microbelts thoroughly.

2.3. Apparatus and electrochemical measurements

UV–vis spectra were recorded on a UV-1700 spectrophotometer (Shimadzu, Japan). FT-IR spectra were obtained on a Nicolet Magna-IR 560 spectrophotometer (Bruker, Germany). The IR spectra were analyzed using the software of Omnic 7.2a from Thermo Electron Corporation. Cyclic voltammetry (CV) measurements were performed on a Model CHI 601C Electrochemical Workstation (CH Instruments, USA). All experiments were conducted using a three-electrode electrochemical cell (10-mL volume with a working volume of 5 mL), with a working electrode (Hb microbelts modified GC electrode or bare GC electrode as the control), an Ag/AgCl, 3 M KCl reference electrode, abbreviated as Ag(RE), and a platinum wire counter electrode. Prior to the electrochemical measurements, all the test solutions were purged with high-purity nitrogen for 20 min and a nitrogen atmosphere was kept over the solution during measurements. For amperometric detection, all measurements were performed by applying an appropriate potential to the working electrode and allowing the transient background current to decay to a steady-state value, before the addition of the analyte (H_2O_2 or NO_2^-). A stirred solution was employed to provide convective transport.

3. Results and discussion

3.1. Characterization of electrospun Hb microbelts

Electrospinning has been widely used to generate various nano- and microstructures. In this study, Hb dissolved in TFE solution was successfully electrospun into Hb microbelts. Fig. 1A and its inset illustrate typical SEM images of the electrospun Hb microbelts with different magnifications. One can see that the electrospun Hb presents a randomly orientated and highly porous three-dimensional microbelts-mesh structure, and the Hb microbelts have an average width of ~2.5 μm and thickness of ~600 nm, and a length up to several millimeters. It can also be seen that the surface of Hb microbelts is smooth. The conformational integrity of electrospun Hb microbelts was further investigated by UV–vis spectroscopy. The position of the Soret absorption band of iron heme groups in Hb can provide structural information about possible denaturation of Hb. As shown in Fig. 1B, the Hb dissolved in buffer solution gives a typical Soret band at 406 nm as expected, while the cast Hb film on glass and the electrospun Hb microbelts show Soret bands at 411 nm. The slight shift in Soret band may be attributed to the interaction among protein molecules in dry status, in which the proteins are much closer to each other than in buffer solution. Such interactions would not destroy the secondary structure of Hb nor change the conformation in the heme group region (Shan et al., 2009). The UV–vis spectra suggest that the electrospinning of Hb in TFE would not change the structure and conformation of Hb. Besides UV–vis spectroscopy, FT-IR spectroscopy is another sensitive method to investigate the secondary structural variation of Hb. Fig. 1C shows the spectra of native Hb powder and electrospun Hb microbelts. The amide I band at 1650 cm^{-1} results from C=O stretching vibrations of the peptide linkage while the amide II band at 1535 cm^{-1} is caused by a combination of N–H in-plane blending and C–N stretching of the peptide groups (Wang et al., 2004; Zhao et al., 2009). As the FT-IR spectra for native Hb powder and electrospun Hb microbelts are similar to each other, the results suggest that Hb in the electrospun microbelts retained the essential features of its native structure.

3.2. Direct electrochemistry of Hb microbelts modified GC electrode

The direct electrochemistry of Hb microbelts modified GC electrode was investigated using CV. Fig. 2A shows the typical CVs obtained from the bare GC electrode and Hb microbelts modified GC electrode in 0.1 M pH 7.0 phosphate buffer. One can see that

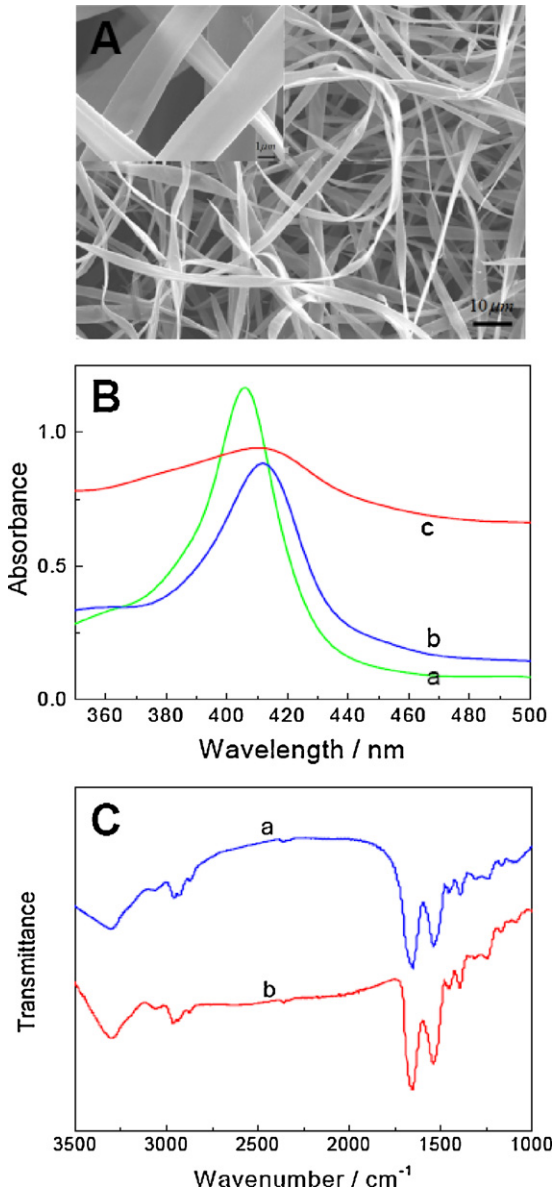

Fig. 1. (A) Typical SEM images of Hb microbelts at low (scale bar = 10 μm) and high (inset, scale bar = 1 μm) magnification; (B) UV–vis spectra of Hb in pH 7.0 phosphate buffer solution (a), dry Hb film cast from Hb aqueous solution (b), and dry Hb microbelts film (c); (C) FT-IR spectra of native Hb powder (a) and electrospun Hb microbelts (b).

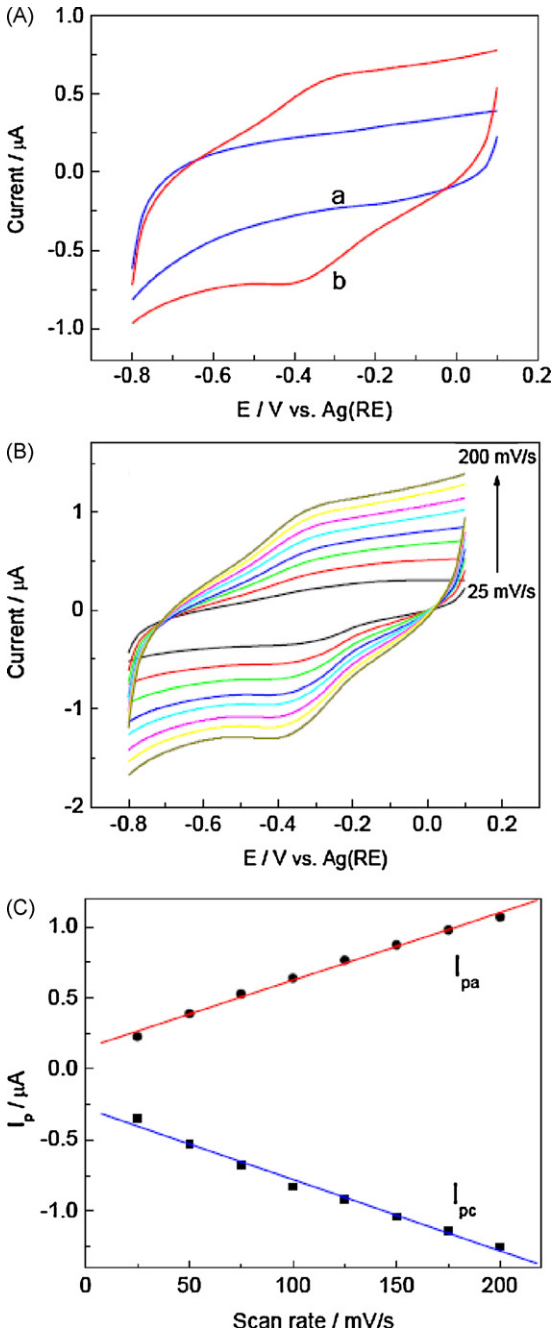

Fig. 2. (A) Cyclic voltammograms of the bare GC electrode (a) and Hb microbelts modified GC electrode (b) in 0.1 M pH 7.0 phosphate buffer solution at a scan rate of 100 mV/s; (B) cyclic voltammograms of Hb microbelts modified GC electrode in 0.1 M pH 7.0 phosphate buffer solution at scan rates of 25, 50, 75, 100, 125, 150, 175 and 200 mV/s, respectively; (C) the plot of peak current versus scan rate.

a pair of well-defined, quasi-reversible redox peaks is observed for the Hb microbelts modified GC electrode (curve b). The anodic peak potential (E_{pa}) and cathodic peak potential (E_{pc}) are located at −0.321 and −0.377 V, respectively, representing the characteristic of Fe(III)/Fe(II) redox couple in the heme groups (Cai and Chen, 2004; Jian et al., 2007). The formal potential ($E^{0'}$) defined as the average of E_{pa} and E_{pc} is −0.349 V, which is in agreement with the reported values in the literature (Cai and Chen, 2004; Jian et al., 2007). The peak-to-peak separation (ΔE_p) is 56 mV at a scan rate of 100 mV/s, which is smaller than 70 mV for Hb immobilized on a sodium alginate-multiwall carbon nanotubes composite film (Zhao et al., 2009), 58.6 mV for Hb in Fe_3O_4 nanoparticle (Cao and Hu, 2006), and 64 mV for Hb in silica sol–gel (Wang et al., 2004) obtained at the same scan rate, indicating more reversible direct electron transfer achieved between Hb and electrode. Such enhanced electrochemical behavior can be attributed to the highly porous three-dimensional architecture and large specific surface area of Hb microbelts and close contact of Hb microbelts to the electrode. As a control, there is no oxidation or reduction peak observed for the bare GC electrode due to the absence of Hb (curve a).

Fig. 2B shows the CVs of Hb microbelts modified electrode in 0.1 M pH 7.0 phosphate buffer solution at different scan rates. The redox peak currents increased linearly with the scan rate in the range from 25 to 200 mV/s (Fig. 2C) with correlation coefficients (R^2) of 0.994 (I_{pa}) and 0.991 (I_{pc}), respectively, indicating that the redox process was a typical quasi-reversible surface-controlled electrochemical process (Shan et al., 2007). It further demonstrates the direct electrochemistry nature of Hb microbelts on the electrode. According to Faraday's laws of electrolysis: $Q = nFA\Gamma^*$, where

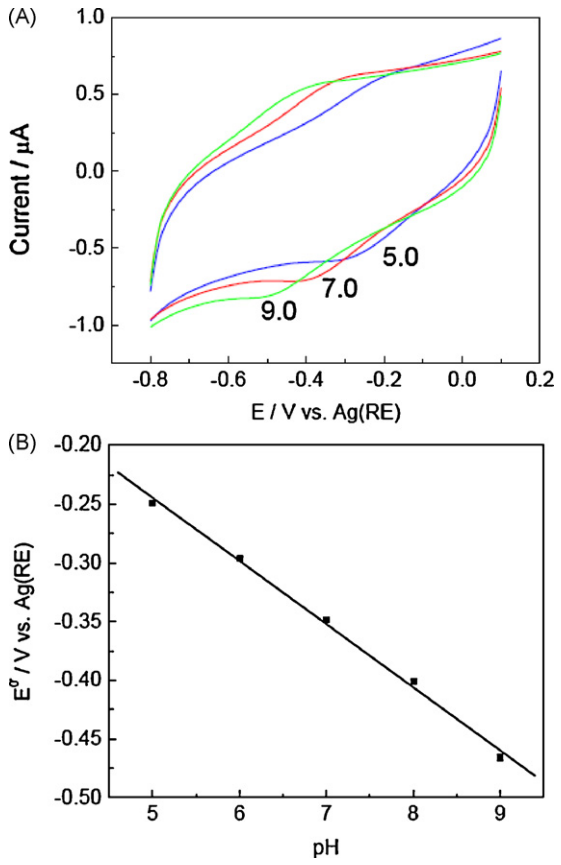

Fig. 3. (A) Cyclic voltammograms of Hb microbelts modified GC electrode in phosphate buffer solutions with different pH values of 5.0, 7.0 and 9.0. Scan rate was set at 100 mV/s; (B) the plot of the formal potential versus pH.

Q (5.7339×10^{-7} C) is the charge involved in the reaction, A is the electrode area, n is the number of electron transferred, F is the Faraday constant, and Γ^* is the surface coverage of the electroactive substance. By integration of reduction peaks, the surface coverage (Γ^*) of electroactive Hb in the microbelts was estimated to be 8.41×10^{-11} mol/cm^2, which is about 4.5 times higher than that of the theoretical monolayer coverage (1.89×10^{-11} mol/cm^2) (Wang et al., 2005). This indicated that multilayer of Hb participated in the electron-transfer process.

As the pH can greatly affect the CVs as well as the redox peak potentials, the pH effect on the direct electrochemistry of Hb was also investigated and presented in Fig. 3A. One can see that an increase in buffer pH caused a negative shift in redox peak potentials of the heme Fe(III)/Fe(II) redox couples. The plot of formal potential ($E^{0'}$) versus pH is presented in Fig. 3B. The decrease of the formal potential with pH shows a linear correlation ($R^2 = 0.997$) with a slope of −53.9 mV/pH, which is close to the Nernstian value of −59.2 mV/pH at room temperature (25 °C) for the reversible one-electron transfer accompanied with single-proton transportation (Zhao et al., 2006a). Thus, the electrochemical oxidation and reduction of Hb can be schematically expressed as follows: Hb heme Fe(III) + H^+ + e^- ↔ Hb heme Fe(II) (Zhao et al., 2006a).

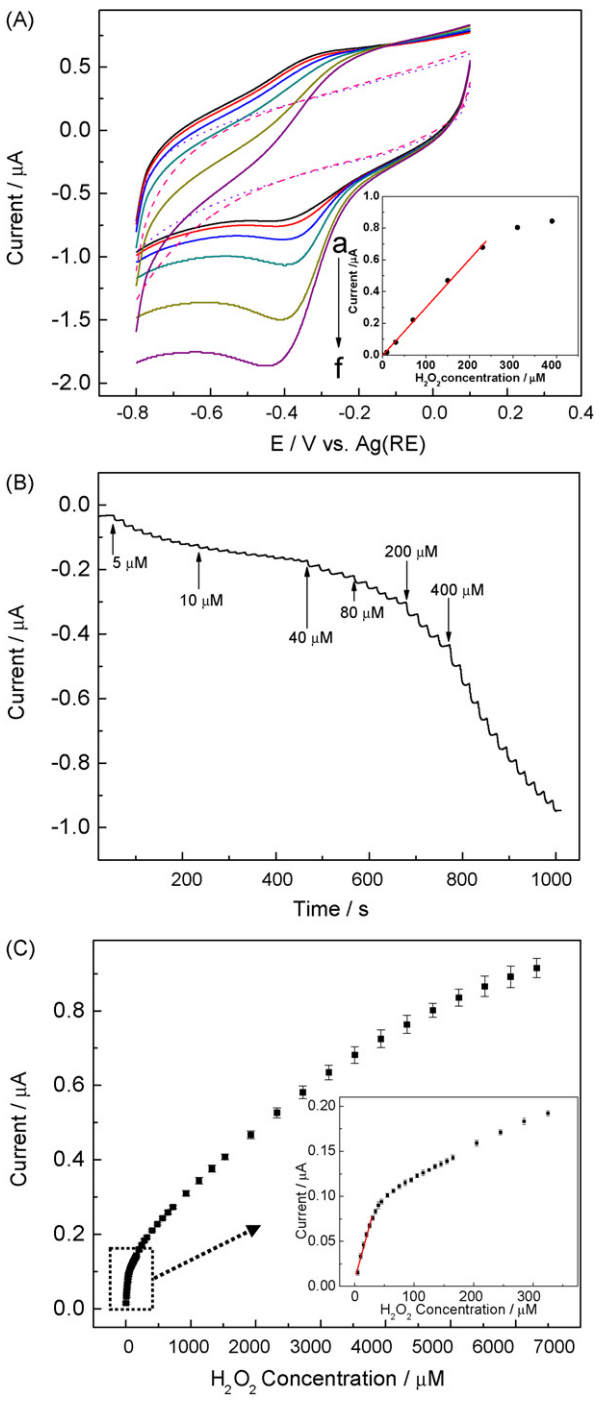

Fig. 4. (A) Cyclic voltammograms of bare GC electrode (dot line: without H_2O_2; dash line: with 70 μM H_2O_2) and cyclic voltammograms of Hb microbelts modified GC electrode at a scan rate of 100 mV/s in pH 7.0 phosphate solution with (a) 0, (b) 10, (c) 30, (d) 70, (e) 150, (f) 230 μM H_2O_2. Inset: the corresponding calibration plot; (B) amperometric response of Hb microbelts modified electrode with successive additions of H_2O_2 to 0.1 M pH 7.0 phosphate buffer solution at an applied potential of −0.377 V; (C) the corresponding calibration plot of amperometric response towards H_2O_2. Inset: enlarged drawing of calibration plot for low H_2O_2 concentrations.

3.3. Hb microbelts modified GC electrode for sensitive H_2O_2 detection

The electrocatalytic property of the as-prepared Hb microbelts modified electrode towards H_2O_2 reduction was investigated by CVs. H_2O_2 was selected as a model compound because the detection of H_2O_2, a product of enzymatic reactions catalyzed by a large number of oxidases (e.g. glucose oxidase and peroxidase), is practically important in the field of biosensor development (Salimi et al., 2007). Fig. 4A presents the CVs in the absence and presence of different H_2O_2 concentrations, recorded at the bare GC electrode and Hb microbelts modified GC electrode. One can see that there is no significant reduction peak observed on the bare GC electrode. However, the obvious reduction peak current obtained on the Hb

Table 1
The summary of recently reported Hb based amperometric H_2O_2 biosensors.

Electrode	Applied potential	Electrolyte, pH	Detection limit (μM)	Reference
Hb microbelts (GC)	−0.377 V (vs. Ag(RE))	0.1 M phosphate, pH 7	0.61	This study
Hb/TiO_2 sol–gel (GC)	−0.3 V (vs. SCE)	0.2 M acetate, pH 4.5	0.12	Yu and Ju (2003)
Hb/undoped nanocrystalline diamond (GC)	−0.3 V (vs. SCE)	0.025 M phosphate, pH 7	0.4	Zhu et al. (2007)
Hb/carbonized TiO_2 nanotubes (GC)	−0.35 V (vs. SCE)	0.1 M acetate, pH 5	0.92	Guo et al. (2008)
Hb/PAN-co-PAA (GC)	−0.25 V (vs. SCE)	0.1 M phosphate, pH 7	4.5	Shan et al. (2009)
Hb/chitosan and nano-$CaCO_3$ (GC)	−0.25 V (vs. SCE)	0.1 M phosphate, pH 7	8.3	Shan et al. (2007)
Hb/sodium alginate-MWCNTs (GC)	−0.4 V (vs. SCE)	0.1 M phosphate, pH 7	16.41	Zhao et al. (2009)

microbelts modified GC electrode increases with increasing concentration of H_2O_2 and shows a linear calibration range for H_2O_2 from 10 to 230 μM with a correlation coefficient (R^2) of 0.998 (inset of Fig. 4A). At higher H_2O_2 concentration, the reduction peak current gradually levels off and follows a saturation behavior due to the saturation of the active sites in Hb, which can be explained by the Michaelis–Menten kinetics.

The superior electrocatalytic ability and easy fabrication makes the as-prepared Hb microbelts an excellent electrochemical sensing platform for H_2O_2 detection. Fig. 4B shows typical amperometric responses of the Hb microbelts modified GC electrode to the successive addition of H_2O_2 at an applied potential of −0.377 V in 0.1 M pH 7.0 phosphate buffer. The working potential was determined from the reduction peak potential of H_2O_2 in Fig. 4A. The corresponding calibration curve is presented in Fig. 4C. The Hb microbelts modified electrode responds rapidly to the changes in H_2O_2 concentration, producing steady-state reduction current within 8 s. The calibration curve is linear up to 2.7×10^{-5} M (the correction coefficient $R^2 = 0.990$), with a sensitivity of 33.97 μA mM^{-1} cm^{-2} and a detection limit of 6.1×10^{-7} M (a signal-to-noise ratio of 3). The high sensitivity can be attributed to the excellent direct electrochemistry behavior of Hb microbelts. In addition, the electrospun Hb microbelts form a highly porous structure and possess high specific surface area, allowing the access of analytes to the active sites of Hb with minimal diffusion resistance. All these features provide a favorable microenvironment for the electrocatalytic reduction of H_2O_2 and thus allow the sensitive detection of H_2O_2 at physiological pH, which makes it more appealing than other Hb based H_2O_2 biosensors operated in acidic condition (Guo et al., 2008; Yu and Ju, 2003). According to the Lineweaver–Burk equation, the apparent Michaelis–Menten constant $K_{M,app}$, a reflection of the enzymatic affinity to substrate, is calculated to be 0.093 mM. This value is much smaller than that of 0.898 mM for Hb in silica sol–gel film (Wang et al., 2004), 0.533 mM for Hb immobilized on sodium alginate-multiwall carbon nanotubes composites film (Zhao et al., 2009) and 0.75 mM for Hb entrapped in composite matrix based on chitosan and $CaCO_3$ nanoparticles (Shan et al., 2007). The small value of $K_{M,app}$ indicates that Hb in microbelts possesses a higher affinity to H_2O_2, which may be attributed to the good biocompatibility, large surface area, and high direct electron-transfer capability of the as-prepared three-dimensional Hb microbelts. The response of the biosensor was reproducible as demonstrated by the low relative standard deviations of 6.37% ($n = 5$) for 10 μM H_2O_2. Additionally, there was a good electrode-to-electrode reproducibility as characterized by a relative standard deviation of 11.72% ($n = 5$) in the response of five biosensors prepared at different times. Furthermore, there is no interference from ascorbic acid (AA) and uric acid (UA) in the detection of H_2O_2 as AA and UA cannot be oxidized at such low applied potential.

Various Hb based biosensors for H_2O_2 have been reported in literature. However, due to the significant dependence of biosensor performance on various parameters such as the applied potential, the solution pH, the composition of supporting electrolyte, and the electrode materials, it is very difficult to compare one biosensor to others. Table 1 summarizes recently reported Hb based amperometric H_2O_2 biosensors with respect to the electrode material, the applied potential, electrolyte, and the detection limit. It can be seen that the performance of the developed biosensor is among the best Hb based H_2O_2 biosensors.

3.4. Hb microbelts modified GC electrode for sensitive nitrite detection

"Nitrate toxicity" is a misnomer because nitrite (NO_2^-), not nitrate (NO_3^-), is poisonous to animals and human beings. Nitrite can be formed as a result of degradation of nitrate fertilizers which are applied to our environment. In addition, the anti-microbial action of nitrite has been recognized for centuries and widely used in the environment, beverages and food products as a preservative. Nitrite can be toxic in high concentrations to animals, including humans (the lethal dose of nitrite for humans ranges from 33 to 250 mg per kg body weight). A principle concern of nitrite is the possible formation of carcinogenic nitrosamines (Linjinsk and Epstein, 1970) in conditions of defined pH and in other conditions similar to those in the mammalian stomach, and also in vitro in gastric juice. Another concern is that passage of nitrite into the bloodstream results in irreversible conversion of hemoglobin to methemoglobin with oxygen uptake and transportation compromised. Currently, nitrite is determined spectrophotometrically by its reaction with sulphanilamide and N-1-naphthylenediamine. However, this method is complicated, time-consuming and also the results are easily interfered by other oxidants or colored substances present in the sample matrix. Therefore, there is a great demand to develop fast, easy-to-use, highly sensitive and selective biosensor for nitrite detection.

The application of the as-prepared Hb microbelts modified GC electrode for the electrocatalytic reduction and amperometric detection of nitrite was also investigated in 0.05 M pH 4.0 BR buffer solution. As shown in Fig. 5A, there is no significant reduction observed on the bare GC electrode when the applied potential is above −0.8 V. However, the significant reduction of nitrite was observed on the Hb microbelts modified electrode. The reduction (cathodic) peak current at ca. −0.65 V increases significantly with the increase of nitrite concentration. The reduction peak may stem from $[Hb\,Fe(II)(NO)^+]^+$ following the possible reaction routes described in Scheme 1S (Mimica et al., 2001; Wang et al., 2004; Yang et al., 2005).

Generally, amperometry is more sensitive than CV, therefore, the nitrite reduction on Hb microbelts modified electrode was explored for an amperometric nitrite biosensor. Fig. 5B displays the amperometric responses of the Hb microbelts based nitrite biosensor for successive addition of nitrite with 5, 10, 40, 80, 200, and 400 μM/step in 0.05 M pH 4.0 BR buffer at an applied potential of −0.65 V under stirring. The biosensor exhibits a rapid and sensitive response to the addition of nitrite. As shown in Fig. 5B, the biosensor shows a prominent response to the addition of 5 μM nitrite, which is attributed to good catalytic property of Hb microbelts. The biosensor achieves 95% of steady-state current in less than 10 s, indicating a fast electron transfer between Hb and elec-

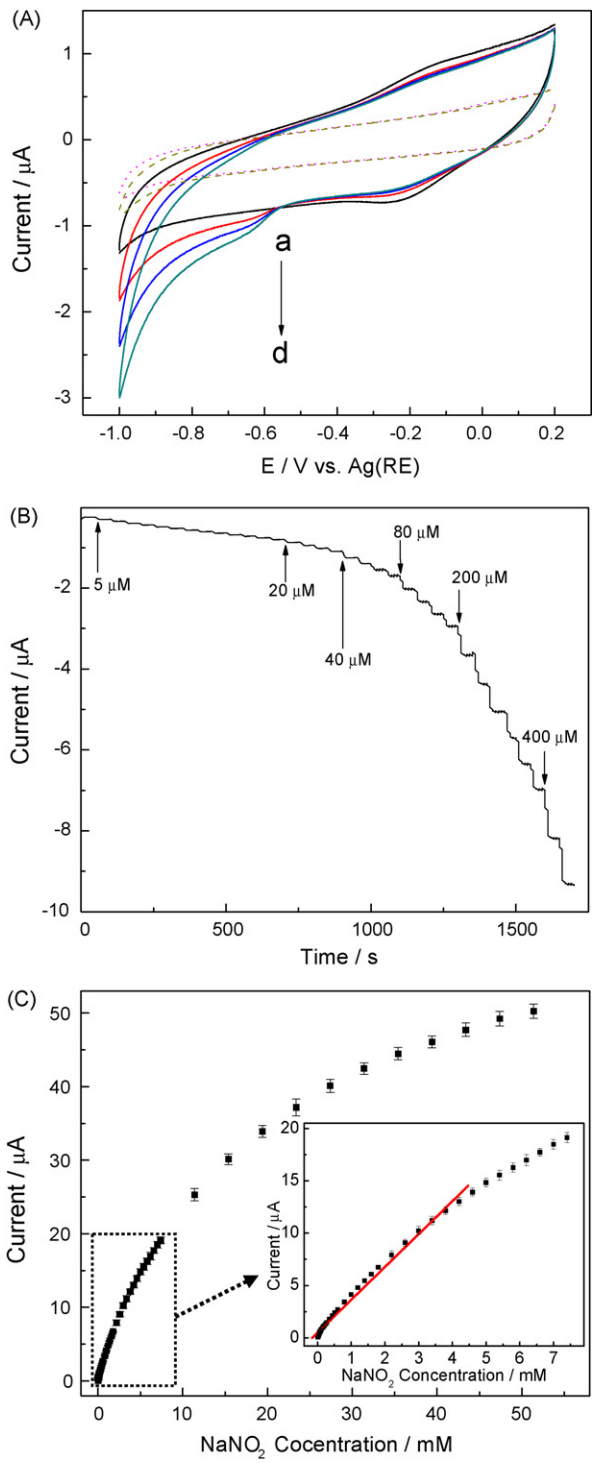

Fig. 5. (A) Cyclic voltammograms of bare GC electrode (dot line: without $NaNO_2$; dash line: with 200 μM $NaNO_2$) and cyclic voltammograms of Hb microbelts modified GC electrode at a scan rate of 100 mV/s in 0.05 M pH 4.0 BR buffer solution with (a) 0, (b) 200, (c) 400, (d) 800 μM $NaNO_2$; (B) amperometric response of Hb microbelts modified electrode with successive additions of $NaNO_2$ to 0.05 M pH 4.0 BR buffer solution at an applied potential of −0.65 V; (C) the corresponding calibration plot of amperometric response towards $NaNO_2$. Inset: enlarged drawing of calibration plot for low $NaNO_2$ concentrations.

trode. The calibration curve of the biosensor is shown in Fig. 5C. The plot shows a linear range up to 4.5×10^{-3} M with a correction coefficient $R^2 = 0.999$. The limit of detection (LOD), determined as 3 times the standard deviation of the signal for buffer (blank), was 4.7×10^{-7} M of nitrite. This value is comparable to or better than most reported values (Dai et al., 2004; Wei et al., 2007). In addition, the $K_{M,app}$ value for nitrite was calculated to be 0.713 mM, more than 10 times smaller than that of 7.48 mM for Hb in titania sol–gel film (Zhao et al., 2006b) and 9.4 mM for Hb entrapped in PVA-ionic liquid (Zhang et al., 2009). The reproducibility of the developed biosensor for nitrite was also investigated. The relative standard deviation of 5.28% ($n = 5$) for 5 μM nitrite demonstrated good intra-electrode reproducibility. Additionally, the good electrode-to-electrode reproducibility was characterized by the low relative standard deviations of 7.43% ($n = 5$) in the response to 5 μM nitrite on five biosensors. Furthermore, the interference study shows that 4 mM NaCl, NaI, KNO_3, Na_2CO_3, and $MgCl_2$ do not interfere with the detection of 20 μM of nitrite. These results should make the biosensor an ideal analytical tool for sensitive detection of nitrite in the environment.

4. Conclusions

In summary, Hb microbelts based biosensor was prepared by directly electrospinning Hb on the surface of GC electrode without using any immobilization matrix. The as-electrospun Hb microbelts were characterized by UV–vis and FT-IR and the results suggested that Hb in the microbelts retains its native structure. The Hb microbelts modified electrode was then applied to study the electrocatalytic reduction of H_2O_2 and nitrite in 0.1 M pH 7.0 phosphate buffer medium and 0.05 M pH 4.0 BR buffer, respectively. Enhanced electrochemical reduction towards H_2O_2 and nitrite was achieved, which may be attributed to the enhanced direct electrochemistry of Hb, and the highly porous structure and large surface of the as-electrospun Hb microbelts. The Hb microbelts based amperometric biosensor shows a fast response to the analytes and has excellent detection limits of 0.61 μM for H_2O_2 and 0.47 μM for nitrite, which are among the best reported values in literature. The biosensor also has a wide dynamic range with respect to the analyte concentration, which follows typical Michaelis–Menten saturation kinetics. This work demonstrates that the electrospun Hb microbelts can significantly improve the direct electrochemistry behavior of Hb and has great potential application in mediator-free biosensor applications.

Acknowledgements

We greatly appreciate the funding from NSF and USGS. YD also thanks the partial support from UConn Center for Environmental Science and Engineering.

Appendix A. Supplementary data

Supplementary data associated with this article can be found, in the online version, at doi:10.1016/j.bios.2010.01.024.

References

Armstrong, F.A., Hill, H.A.O., Walton, N.J., 1988. Acc. Chem. Res. 21, 407–413.
Cai, C.X., Chen, J., 2004. Anal. Biochem. 325, 285–292.
Cai, W.Y., Feng, L.D., Liu, S.H., Zhu, J.J., 2008. Adv. Funct. Mater. 18, 3127–3136.
Cao, D.F., Hu, N.F., 2006. Biophys. Chem. 121, 209–217.
Dai, Z., Liu, S., Ju, H., Chen, H., 2004. Biosens. Bioelectron. 19, 861–867.
Ding, B., Wang, M.R., Yu, J.Y., Sun, G., 2009. Sensors 9, 1609–1624.
Gao, R., Shangguan, X., Qiao, G., Zheng, J., 2008. Electroanalysis 20, 2537–2542.
Guo, C., Hu, F., Li, C.M., Shen, P.K., 2008. Biosens. Bioelectron. 24, 819–824.
Han, X., Huang, W., Jia, J., Dong, S., Wang, E., 2002. Biosens. Bioelectron. 17, 741–746.
He, X.Y., Zhu, L., 2006. Electrochem. Commun. 8, 615–620.
Jia, W.Z., Su, L., Ding, Y., Schempf, A., Wang, Y., Lei, Y., 2009. J. Phys. Chem. C 113, 16402–16407.
Jian, F., Qiao, Y., Zhuang, R., 2007. Sens. Actuators B: Chem. 124, 413–420.
Kapoor, S., Mandal, S.S., Bhattacharyya, A.J., 2009. J. Phys. Chem. B 113, 14189–14195.
Linjinsk, W., Epstein, S.S., 1970. Nature 225, 21–23.
Liu, H.H., Tian, Z.Q., Lu, Z.X., Zhang, Z.L., Zhang, M., Pang, D.W., 2004. Biosens. Bioelectron. 20, 294–304.

Liu, Y., Liu, H.Y., Hu, N.F., 2005. Biophys. Chem. 117, 27–37.
Maduralveeran, G., Ramaraj, R., 2007. J. Electroanal. Chem. 608, 52–58.
Mimica, D., Zagal, J.H., Bedioui, F., 2001. J. Electroanal. Chem. 497, 106–113.
Qiao, Y.B., Jian, F.F., Bai, Q., 2008. Biosens. Bioelectron. 23, 1244–1249.
Salimi, A., Hallaj, R., Soltanian, S., Mamkhezri, H., 2007. Anal. Chim. Acta 594, 24–31.
Shan, D., Cheng, G.X., Zhu, D.B., Xue, H.G., Cosnier, S., Ding, S.N.A., 2009. Sens. Actuators B: Chem. 137, 259–265.
Shan, D., Wang, S.X., Xue, H.G., Cosnier, S., 2007. Electrochem. Commun. 9, 529–534.
Sun, H., Hu, N.F., Ma, H.Y., 2000. Electroanalysis 12, 1064–1070.
Wang, Q.L., Lu, G.X., Yang, B.J., 2004. Biosens. Bioelectron. 19, 1269–1275.
Wang, S.F., Chen, T., Zhang, Z.-L., Shen, X.-C., Lu, Z.-X., Pang, D.-W., Wong, K.-Y., 2005. Langmuir 21, 9260–9266.
Wang, Y., Jia, W.Z., Strout, T., Ding, Y., Lei, Y., 2009a. Sensors 9, 6752–6763.
Wang, Y., Jia, W.Z., Strout, T., Schempf, A., Zhang, H., Li, B.K., Cui, J.H., Lei, Y., 2009b. Electroanalysis 21, 1432–1438.
Wei, S., Dandan, W., Ruifang, G., Kui, J., 2007. Electrochem. Commun. 9, 1159–1164.
Yang, W.W., Bai, Y., Li, Y.C., Sun, C.Q., 2005. Anal. Bioanal. Chem. 382, 44–50.
Yoon, J., Jung, Y.S., Kim, J.M., 2009. Adv. Funct. Mater. 19, 209–214.
Yu, J.H., Ju, H.X., 2003. Anal. Chim. Acta 486, 209–216.
Zhang, L., 2008. Biosens. Bioelectron. 23, 1610–1615.
Zhang, Y.F., Yan, R., Zhao, F.Q., Zeng, B.Z., 2009. Colloid Surf. B: Biointerf. 71, 288–292.
Zhao, H.Y., Zheng, W., Meng, Z.X., Zhou, H.M., Xu, X.X., Li, Z., Zheng, Y.F., 2009. Biosens. Bioelectron. 24, 2352–2357.
Zhao, S., Zhang, K., Bai, Y., Yang, W.W., Sun, C.Q., 2006a. Bioelectrochemistry 69, 158–163.
Zhao, S., Zhang, K., Sun, Y.Y., Sun, C.Q., 2006b. Bioelectrochemistry 69, 10–15.
Zhao, X.J., Mai, Z.B., Kang, X.H., Zou, X.Y., 2008. Biosens. Bioelectron. 23, 1032–1038.
Zhu, J.T., Shi, C.G., Xu, J.J., Chen, H.Y., 2007. Bioelectrochemistry 71, 243– 248.